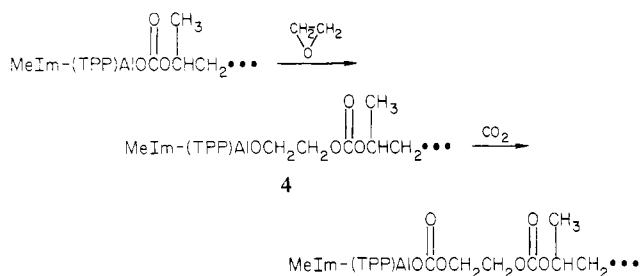
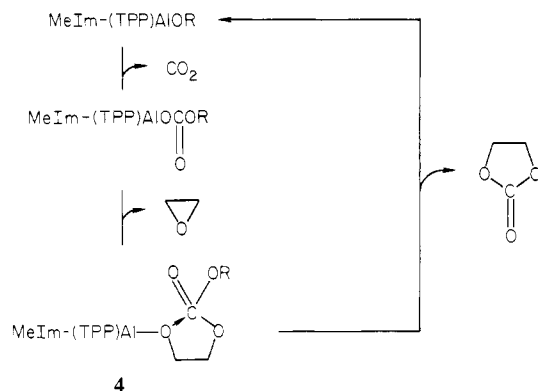


Scheme IV



Scheme V



appeared again and ethylene carbonate was additionally formed (Figure 6, 5 and 6). In conformity with this observation, the  $^1\text{H}$  NMR spectrum of the reaction system with a sufficient amount of  $\text{CO}_2$  (Figure 8) showed a doublet signal ( $\text{o}$ ,  $\delta -0.5$ ) corresponding to the "trapped  $\text{CO}_2$ " (see Figure 4), while the signal at  $\delta -2.3$  due to the starting alkoxide was not observed. Therefore,

(tetraphenylporphinato)aluminum alkoxide reproduced as the result of the cyclic carbonate formation may react instantaneously with the dissolved  $\text{CO}_2$  to serve again the "trapped  $\text{CO}_2$ " for the repeated reaction, as long as a sufficient amount of  $\text{CO}_2$  exists in the reaction system.

It should be noted here that the  $^1\text{H}$  NMR spectrum of the (TPP)AlPPO-MeIm- $\text{CO}_2$ -ethylene oxide system (Figure 8) also shows a triplet signal ( $\text{p}$ ) assignable to the structure MeIm-(TPP)Al-O-CO-O- $\text{CH}_2$ - $\text{CH}_2$ ... (see Figure 5,  $\text{k}''$ ). Together with the fact that an infrared absorption due to linear carbonate linkage is observed at  $1740\text{ cm}^{-1}$  in this system (Figure 6), the reaction in Scheme IV is considered also to take place. Thus the participation of linear carbonate as the intermediate is indicated in the formation of cyclic carbonate.<sup>12</sup> As illustrated in Scheme V, cyclic carbonate is considered to be formed at least partly, by the intramolecular nucleophilic attack of aluminum alkoxide group on the adjacent linear carbonate linkage of **4**.

### Conclusion

The fixation reaction of carbon dioxide with a (porphinato)-aluminum alkoxide was first investigated by the spectroscopic methods using (tetraphenylporphinato)aluminum alkoxide having a long oxyalkylene chain as an alkoxide group, taking advantage of the good solubility. This alkoxide with unique structure was found to behave as a "carrier" of carbon dioxide activated enough to react under mild conditions with epoxide in the presence of 1-methylimidazole to afford cyclic carbonate.

**Registry No.** **1c**, 71102-37-9; **1d** ( $\text{R} = \text{Me}$ ), 84279-80-1; **1d** ( $\text{R} = \text{H}$ ), 84279-82-3; **1d** ( $\text{R} = t\text{-Bu}$ ;  $n = 1$ ), 84279-77-6; MeIm(TPP)Al-( $\text{OC}_6\text{H}_5$ ) $_n\text{OH}$ , 84279-81-2; MeIm(TPP)Al( $\text{OCH}_2\text{CH}_2$ ) $_n\text{OH}$ , 84279-83-4; MeIm(TPP)AlOCH( $\text{CH}_2\text{Cl}$ )C( $\text{CH}_3$ ) $_3$ , 84279-78-7; MeIm(TPP)AlPPO- $\text{CO}_2$ , 84332-50-3; MeIm(TPP)AlPEO- $\text{CO}_2$ , 84279-79-8; *tert*-butylene oxide, 2245-30-9; ethylene oxide, 75-21-8; propylene oxide, 75-56-9; carbon dioxide, 124-38-9; 1-methylimidazole, 616-47-7; ethylene carbonate, 96-49-1; propylene carbonate, 108-32-7; carbonic acid, 463-79-6.

## Photochemistry of Diastereomeric 2,4-Diphenylpentan-3-ones and Related Ketones in "Super-Cage" Environments Provided by Micelles, Porous Glass, and Porous Silica: Temperature and Magnetic Field Effects

Bruce H. Baretz and Nicholas J. Turro\*

Contribution from the Chemistry Department, Columbia University, New York, New York 10027. Received April 26, 1982

**Abstract:** The photochemistry of the meso and *d,l* isomers of 2,4-diphenylpentan-3-one (DPP), of 1,3,4-triphenylbutan-2-one (TPB), and of 1,3-diphenylbutan-2-one ( $\alpha$ -MeDBK) has been investigated in homogeneous solvents and in "super-cage" environments that impose constraints on the diffusional displacements of the components of geminate radical pairs and thereby enhance the efficiency of cage reactions of geminate pairs. Solutions of ionic detergents containing micelles, porous glass, and porous silica provide examples of such super-cage environments. The major course of reaction in the photolysis of DPP in pentane or benzene is decarbonylation followed by coupling ( $\approx 93\%$ ) or disproportionation ( $\approx 3\%$ ) of PhCHCH $_3$  radicals. In super-cage environments, the extent of disproportionation increases significantly, as does diastereomeric interconversion. Although temperature effects (in the range 25 to  $-77\text{ }^\circ\text{C}$ ) on the product of DPP are small for photolysis in homogeneous solution, substantial variations in product ratios with variation in temperature can be achieved when the photolyses are conducted in super-cage environments. Similarly, although magnetic field effects on the product distributions are negligibly small for photolysis in homogeneous solutions, significant variations are found for photolysis of DPP in super-cage environments. The general features of the results with DPP are analogous to those observed for photolysis of TPB and  $\alpha$ -MeDBK. A scheme based on the established photochemistry of dibenzyl ketone is proposed which provides a working mechanism that is consistent with all of the observations of this investigation.

The homolytic  $\alpha$  cleavage (type I) of ketones is among the most scrutinized of organic photoreactions.<sup>1</sup> The paradigm mechanism

for  $\alpha$  cleavage of a ketone involves photoexcitation to a singlet state followed by intersystem crossing to an  $n,\pi^*$  triplet,  $^3\text{RCOR}$ ,

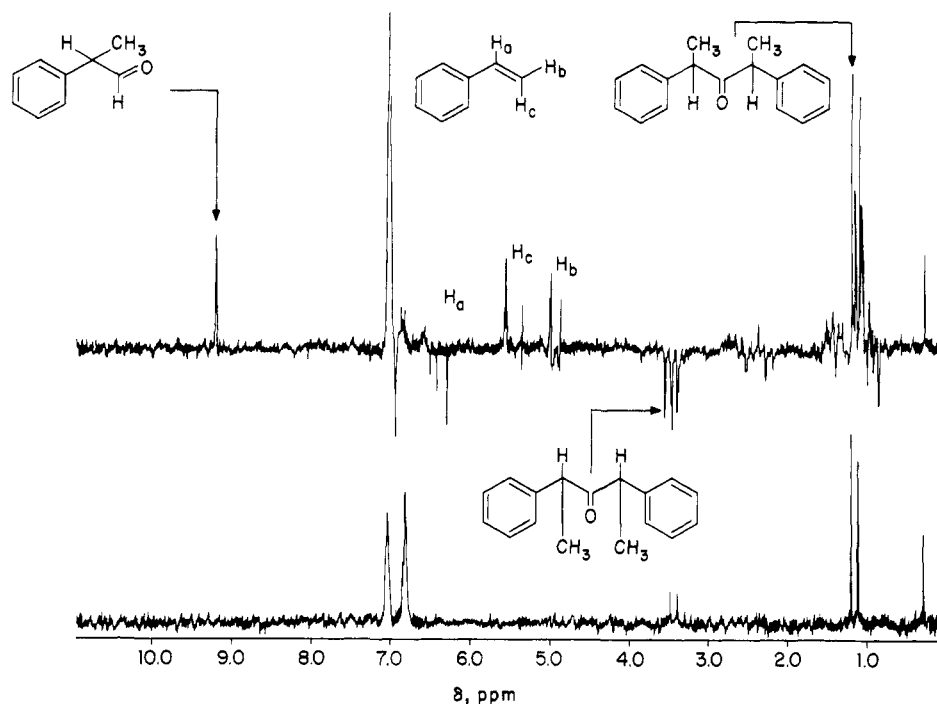


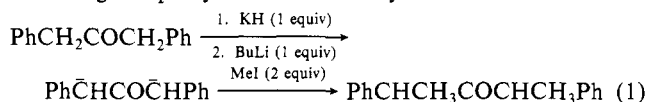
Figure 1. CIDNP spectrum obtained with irradiation of *meso*-DPP in benzene- $d_6$ : (top) irradiated spectrum; (bottom) dark spectrum after irradiation.

which undergoes  $\alpha$  cleavage to produce a geminate triplet radical pair,<sup>3</sup> (RCO  $\dot{R}$ ). The latter serves as the initial precursor to primary cage products, random cage products, and products of scavenging. Considerable research has been directed toward the determination of the dynamics of the various steps and the nature and efficiencies of ketone disappearance and product formation. Although kinetic data appear to compel the conclusion that  $\alpha$  cleavage often occurs with unit efficiency, the quantum yield for net reaction is typically less than one.<sup>2</sup> The inefficiency in net reaction has been attributed to recombination of a sizable fraction of the geminate RCO  $\dot{R}$  pairs to regenerate the ground state of the parent ketone. Evidence for this conclusion is available from CIDNP investigations,<sup>3</sup> from photoepimerization<sup>4</sup> and photoracemization<sup>5</sup> studies, and from <sup>13</sup>C enrichment experiments.<sup>6</sup>

We have investigated the photochemistry of *d,l*- and *meso*-2,4-diphenylpentan-3-one (DPP) and related ketones with respect to the influence of environmental, temperature, and magnetic field effects on the observed products. In particular, the extent of stereoisomerization of the starting ketone and of disproportionation relative to combination of radical pairs were examined to determine the behavior of the geminate radical pair produced by initial  $\alpha$  cleavage.

## Results

A diastereomeric mixture of *d,l*- and *meso*-DPP was synthesized according to eq 1 by addition of methyl iodide to the dianion of



(1) Turro, N. J. "Modern Molecular Photochemistry", Benjamin/Cummings: Menlo Park, CA, 1978; pp 528-534.

(2) Lewis, F. D.; Lauterbach, R. T.; Heine, H. G.; Hartmann, W.; Rudolph, H. *J. Am. Chem. Soc.* **1975**, *97*, 1519.

(3) See, for example: Closs, G. L. In "Chemically Induced Magnetic Polarization"; Wiley: New York, 1973; pp 95-136.

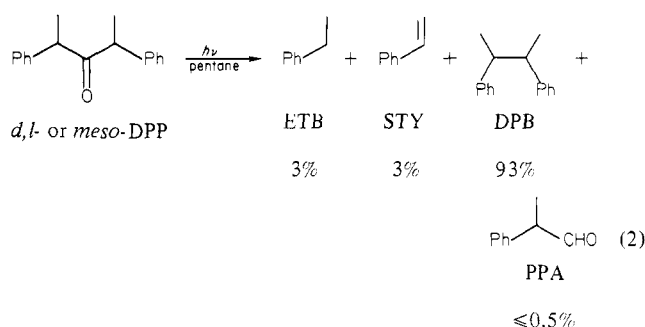
(4) Alumbaugh, R. L.; Pritchard, G. O.; Rickburn, B. *J. Phys. Chem.* **1965**, *69*, 3225. Frey, H. M.; Lister, D. H. *J. Chem. Soc. A* **1970**, 727. Baltrop, J. A.; Coyle, J. D. *J. Chem. Soc. D* **1969**, 1081.

(5) Lewis, F. D.; Magyar, J. G. *J. Am. Chem. Soc.* **1973**, *95*, 5973.

(6) Turro, N. J.; Chow, M.-F.; Chung, C.-J.; Kraeutler, B. *J. Am. Chem. Soc.* **1981**, *103*, 3886. Turro, N. J. *Pure Appl. Chem.* **1981**, *53*, 259. Turro, N. J.; Kraeutler, B. *Acc. Chem. Res.* **1980**, *13*, 369. Kraeutler, B.; Turro, N. *J. Chem. Phys. Lett.* **1980**, *70*, 266. Turro, N. J.; Kraeutler, B.; Anderson, D. R. *Tetrahedron Lett.* **1980**, *21*, 3. Turro, N. J.; Anderson, D. R.; Kraeutler, B. *J. Am. Chem. Soc.* **1979**, *101*, 7435.

dibenzyl ketone (DBK).<sup>7</sup> The *d,l* and *meso* diastereomers were separated by reverse-phase HPLC. The structures of the diastereomers were established by reduction to 2,4-diphenylpentane and correlation with the known *d,l* and *meso* diastereomers of the latter.<sup>8</sup>

**Photochemistry of DPP in Homogeneous Solutions.** Irradiation of *meso*-DPP or *d,l*-DPP in pentane or benzene (1-10 mM) at ambient temperature produces the disproportionation and combination products expected of initial homolytic  $\alpha$  cleavage followed by decarbonylation and reaction of PhCHCH<sub>3</sub> radicals. The products and chemical yields are given in eq 2. The quantum



yield for product formation was 0.62. The major product, 2,3-diphenylbutane (DPB), was a 1:1 mixture of *d,l* and *meso* stereoisomers, starting from either the isomerically pure *d,l*-DPP or *meso*-DPP. Low yields (5%) of a compound that has characteristics (GC/MS analysis) of an isomer of DPB was also produced. The product distribution was essentially the same at 27 or -77 °C in pentane (Table I).

From CIDNP spectroscopy (Figure 1) of the photolysis of DPP in benzene- $d_6$ , it is clear that some of the geminate triplet radical pairs PhCHCH<sub>3</sub>COCHCH<sub>3</sub>Ph produced by  $\alpha$  cleavage undergo cage recombination to yield the initial ketone and its stereoisomer. However, analysis of the product mixture by VPC demonstrates that diastereomeric interconversion accounts for less than  $\approx 1\%$  of the reacted ketone. In addition, significant polarization due

(7) Hauser, C. R.; Harris, T. M. *J. Am. Chem. Soc.* **1959**, *81*, 1154.

(8) Overberger, C. G.; Bonsignore, P. V. *J. Am. Chem. Soc.* **1958**, *80*, 5427. Moritania, T.; Fujiwara, Y. *J. Chem. Phys.* **1973**, *59*, 1175.

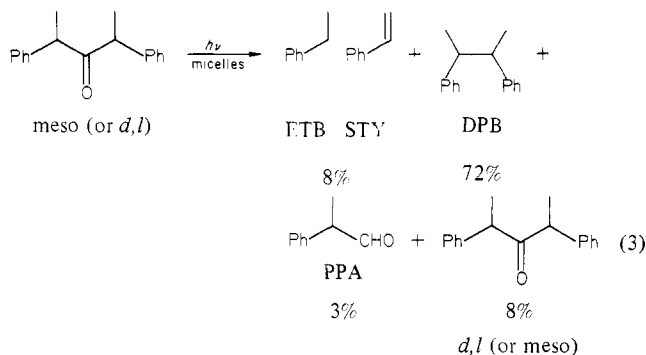
Table I. Product Formation from Photolysis of *meso*-DPP under Various Conditions

product	temp, °C	pentane, <sup>a</sup> %	SDS, <sup>b</sup> %	porous glass, <sup>c</sup> %	porous silica, <sup>d</sup> %	TLC, <sup>e</sup> %	RPTLC, <sup>e</sup> %
<i>d,l</i> -DPP	27	≤0.5 <sup>f</sup>	8	8	8	12	5
<i>d,l</i> -DPP	-77 <sup>g</sup>	≤0.5		45		40	39
DPB	27	93	72	76	83	78	81
DPB	-77 <sup>g</sup>	90		15		31	21
PPA	27	≤0.5	3	2	1	2	2
PPA	-77 <sup>g</sup>	≤0.2		15		12	15
ETB	27	3	9	8	3	3	5
ETB	-77 <sup>g</sup>	4		5		2	5
STY	27	3	8	6	5	5	7
STY	-77 <sup>g</sup>	5		20		15	20

<sup>a</sup> 1 mM solution. <sup>b</sup> 1 mM in 50 mM SDS. <sup>c</sup> To each piece of porous glass was added *meso*-DPP ( $1.3 \times 10^{-6}$  mol) in 100  $\mu$ L of benzene. <sup>d</sup> To porous silica (10 mg) was added *meso*-DPP ( $0.6 \times 10^{-6}$  mol) in 0.6 mL of benzene. The sample was dried under a nitrogen stream, transferred to a clean tube, and sealed under vacuum. <sup>e</sup> To pre-cut TLC and RPTLC plates was added *meso*-DPP ( $0.8 \times 10^{-6}$  mol) in 50  $\mu$ L of benzene. <sup>f</sup> All values are reproducible to within at least 10% of their reported magnitude, except for values less than 1% (which indicate upper limits only). <sup>g</sup> For the silicate samples, the temperature stated refers to that of the bath the samples were immersed in.

to 2-phenylpropionaldehyde (PPA) is observed in the CIDNP spectrum; yet, by VPC analysis, it accounts for less than  $\approx 1\%$  of the total photoproducts.

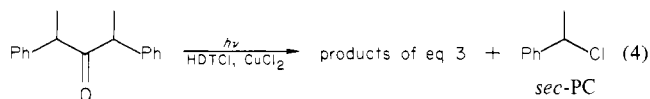
**Photochemistry of DPP in Aqueous Micellar Solutions.** Photolysis of DPP in aqueous solutions of SDS (sodium dodecyl sulfate) or HDTCl (hexadecyltrimethylammonium chloride) at ambient temperature produces products (eq 3 and Table I) similar



to those formed in photolysis in homogeneous solution, with the important differences that (a) significant ( $\approx 8\%$ ) stereoisomerization occurs and (b) measurable ( $\approx 3\%$ ) formation of PPA is observed. The quantum yields for ketone disappearance are 0.50 and 0.33 in HDTCl and SDS solutions, respectively.

The percent stereoisomerization relative to the percent conversion was plotted (Table II) in order to compare the extent of stereoisomerization. The slope,  $s$ , of such a plot provides a reliable measure of the fraction of reacted DPP that undergoes isomerization. For example,  $s = 0.01$  for photolysis of either *d,l*-DPP or *meso*-DPP in benzene or pentane: i.e., the extent of photoisomerization relative to the net reacting ketone is of the order of 1%. In contrast,  $s = 0.10$  for photolysis of either *d,l*-DPP or *meso*-DPP in SDS or HDTCl micellar solution; i.e., a significant ( $\approx 10\%$ ) quantity of the reacted ketone undergoes stereoisomerization.

The influence of paramagnetic gengenions on the values of  $s$  was examined by addition of  $\text{Eu}^{3+}$  (as  $\text{EuCl}_3$ ) and of  $\text{Cu}^{2+}$  (as  $\text{CuCl}_2$ ) to SDS and HDTCl solutions of DPP, respectively. In the case of addition of  $\text{Cu}^{2+}$ , a new product, *sec*-phenethyl chloride (PC) appeared (eq 4).



Both the yield of photoisomerization and the yield of PC were influenced by application of a magnetic field of 3000 G. The former yield decreased by 40% and the latter yield increased by 600% over the values observed with irradiations at 0 G.

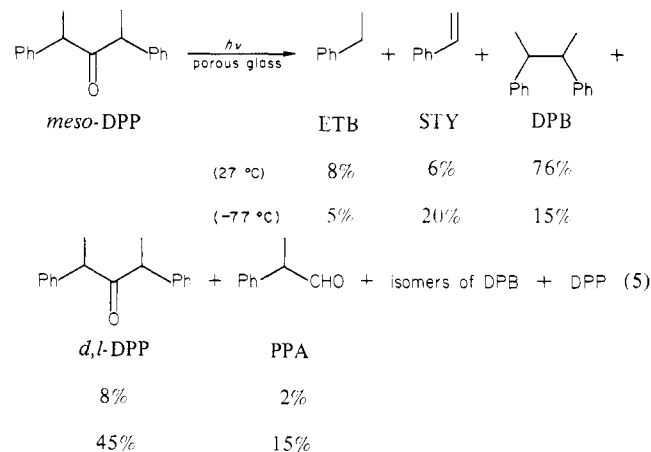
**Photochemistry of *meso*-DPP on Porous Glass.** Photolysis of *meso*-DPP on porous Vycor glass (Corning borosilicate glass no.

Table II. Isomerization Efficiency Slopes at Ambient Temperature

2,4-DPP	environment	$H$ , kG	slope <sup>a</sup>
<i>d,l</i>	SDS <sup>c</sup>	0	0.14
<i>d,l</i>	HDTBr	0	0.09
<i>d,l</i>	HDTCl	0	0.08
<i>meso</i>	SDS	0	0.15
<i>meso</i>	SDS	3	0.10
<i>meso</i>	HDTCl	0	0.11
<i>meso</i>	HDTCl	3	0.07
<i>meso</i>	SDS/ $\text{EuCl}_3$ <sup>d</sup>	0	0.11
<i>meso</i>	SDS/ $\text{EuCl}_3$	3	0.09
<i>meso</i>	HDTCl/ $\text{CuCl}_2$	0	0.10
<i>meso</i>	porous glass <sup>e</sup>	0	0.17
<i>meso</i>	porous glass	3	0.12

<sup>a</sup> Slopes are obtained from the plots described below.<sup>f</sup> Error limits are  $\leq 0.01$ . <sup>b</sup> All ketone concentrations in micelle solutions are 1 mM. <sup>c</sup> Detergent concentrations are 50 mM for SDS and HDTCl and 25 mM for HDTBr. Solutions were  $\text{N}_2$  purged before irradiation. <sup>d</sup> Metal concentrations are 10 mM. <sup>e</sup> To each piece of porous glass was added *meso*-DPP ( $1.3 \times 10^{-6}$  mol) in 100  $\mu$ L of benzene. <sup>f</sup> The percent isomer, the ordinate, expressed as, for example,  $[\textit{d,l}\text{-DPP}]/([\textit{d,l}\text{-DPP}] + [\textit{meso}\text{-DPP}])$  when *meso*-DPP is the starting ketone being irradiated. The abscissa is expressed as  $([\textit{d,l}\text{-DPB}] + [\textit{meso}\text{-DPB}] + [\textit{sec}\text{-PC}])/([\textit{d,l}\text{-DPP}] + [\textit{meso}\text{-DPP}] + [\textit{sec}\text{-PC}])$  when *meso*-DPP is the starting ketone. As such, the slopes, in general, overestimate the percentage of photoisomer formed relative to total photoproducts.

7930) at ambient temperature produces the same products as observed in micellar solutions (eq 5). The extent of isomerization



is somewhat increased ( $s = 0.17$ ) relative to that observed in micellar solution ( $s = 0.10\text{--}0.15$ ); in addition, a magnetic field effect is observed on the extent of photoisomerization (Table II).

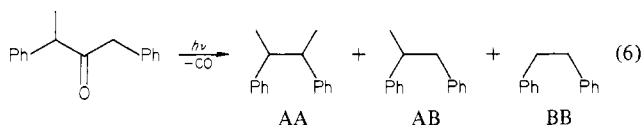
**Table III.** Magnetic Field Effects on Cage Reactions of Benzyl-*sec*-Phenethyl Radical Pairs in Micelles and Silicate Surfaces

environment	cage value			magnetic field effect, %
	temp, °C	<i>H</i> = 0 kG, %	<i>H</i> = 3 kG, %	
HDTCl <sup>a</sup>	27	71 <sup>e</sup>	52	-27
SDS <sup>b</sup>	27	74	50	-32
porous glass <sup>c</sup>	27	38	15	-61
TLC <sup>d</sup>	27	9	6	-32
TLC	-77 <sup>f</sup>	29	19	-36
RPTLC <sup>d</sup>	27	15	11	-26
RPTLC	-77 <sup>f</sup>	47	27	-43

<sup>a</sup> 1 mM in 50 mM HDTCl. <sup>b</sup> 1 mM in 50 mM SDS. <sup>c</sup> Porous glass was soaked in a benzene solution of  $\alpha$ -MeDBK (10 mM), removed, and then vacuum dried. <sup>d</sup> To pre-cut TLC and RPTLC was added  $\alpha$ -MeDBK ( $4.3 \times 10^{-6}$  mol) in 50  $\mu$ L of benzene. <sup>e</sup> All values are reproducible to within at least 5% of their reported magnitude. <sup>f</sup> Refers to the temperature of the bath in which the samples were immersed.

A rather dramatic increase in photoisomerization was observed upon lowering the reaction temperature to -77 °C (45% of total photoproducts). In addition to the observation of a substantial increase in the yield of PPA at -77 °C, minor products tentatively identified as isomers of DPP and DPB were noted.

**Photochemistry of 1,3-Diphenylbutan-2-one in Micelles, Pentane, and on Porous Glass.** The extent of recombination of geminate radical pairs that result from decarbonylation was investigated in a series of experiments with the asymmetrical ketone 1,3-diphenylbutan-2-one ( $\alpha$ -MeDBK). In this system, the ratio of three products (AA:AB:BB) resulting from the coupling of PhCH<sub>2</sub>PhCHCH<sub>3</sub> radical (eq 6) provides a measure of "cage" recombination of geminate PhCH<sub>2</sub>PhCHCH<sub>3</sub> radical pairs.



The "cage effect" (yield of geminate radical pair combinations relative to reacted ketone) in pentane is 0%. The "cage effect" for  $\alpha$ -MeDBK in SDS (HDTCl) micelles is 74% (71%) at 0 G and 50% (52%) in a field of 3000 G (Table III). Irradiation of  $\alpha$ -MeDBK adsorbed to porous glass leads to a cage effect at 0 G of 38%. At 3000 G, the cage drops to 15%.

**Photochemistry of *meso*-DPP on Porous Silica.** Photolysis of *meso*-DPP at ambient temperature on porous silica (surface area 209 m<sup>2</sup> per g, mean pore diameter 122 Å) produces a product distribution that is qualitatively similar to that produced by photolysis on porous glass (i.e., eq 5).

**Photolysis of *meso*-DPP on Silica Gel (TLC Plates).** Photolysis of *meso*-DPP at ambient temperature on silica gel was performed by irradiating TLC plates that had been impregnated with DPP and then dried under vacuum. The product distribution (as well as a temperature effect on this distribution) obtained was qualitatively similar to that observed in the photolysis on porous glass and porous silica (i.e., eq 5).

In a similar fashion, photolysis of  $\alpha$ -MeDBK on TLC was investigated (Table III). In the earth's field, the cage effect (eq 6) was found to be 9% and 29% at ambient temperature and -77 °C, respectively. In a field of 3000 G, the cage effect was 6% and 19% at ambient temperature and -77 °C, respectively. Phenylacetaldehyde (PAA), a product not observed in homogeneous solution irradiation, is produced in a significant amount ( $\approx$ 5%). The yield of PAA is enhanced at -77 °C.

**Photolysis of *meso*-DPP on Reverse-Phase Silica Gel (RPTLC Plate).** Silica gel that is derivatized with alkylsilanes was employed for preparing "reverse-phase" TLC (RPTLC) plates. Photolysis of *meso*-DPP on RPTLC plates in the earth's field at ambient temperature resulted in a product distribution (as well as a temperature effect on this distribution) that is qualitatively similar

**Table IV.** Stilbene Formation with Photolysis of 1,3,4-TPB under Different Conditions<sup>a</sup>

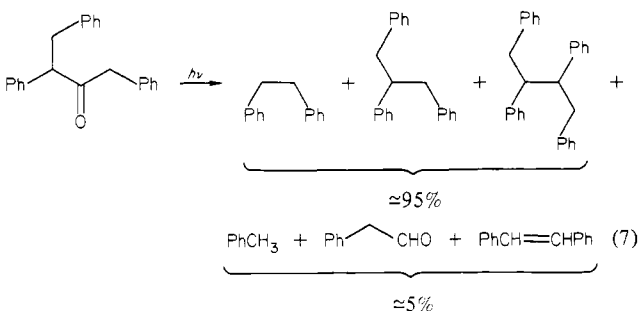
environment	temp, °C	% stilbene <sup>b</sup>	% DPES <sup>c</sup>	% cage <sup>d</sup>
HDTCl	27	6 <sup>f</sup>	94	56
benzene	27	3	97	0
porous glass	27	4	96	51
porous glass	-77 <sup>g</sup>	24	76	56
silica <sup>e</sup>	-77 <sup>g</sup>	19	81	79
2-THF	-77	7	93	0
solid state	-77	2	98	98

<sup>a</sup> 1,3,4-TPB is 1,3,4-triphenylbutan-2-one. <sup>b</sup> % stilbene is defined as 100 - % DPES. <sup>c</sup> The three diphenylethanes (1,2-diphenylethane, 1,2,3-triphenylpropane, and the diastereomeric 1,2,3,4-tetraphenylbutane) recovered relative to all photoproducts. <sup>d</sup> The percent of 1,2,3-triphenylpropane formed within a radical-pair cage. <sup>e</sup> Commercial chromatographic grade silica, Baker 60-240 mesh. <sup>f</sup> All values are reproducible to within at least 10% of their reported magnitude. <sup>g</sup> Refers to the temperature of the bath in which the samples were immersed.

to that produced by photolysis of TLC plates (i.e., eq 5).

Photolysis of  $\alpha$ -MeDBK on RPTLC plates in the earth's field at ambient temperature and at -77 °C resulted in cage effects of 15% and 47%, whereas in a field of 3000 G, the cage effect was 11% and 27%, respectively (Table III).

**Photochemistry of 1,3,4-Triphenylbutan-2-one (TPB).** Photolysis of TPB in the earth's field at ambient temperature in benzene, in HDTCl micelles, or on porous glass and silica gel results mainly in combination products with small yields of disproportionation products (eq 7). The yield of disproportionation products increases to 20-25% at -77 °C for porous glass or silica gel photolysis (Table IV).



Crystalline TPB was photolyzed at -77 °C and yielded 98% 1,2,3-triphenylpropane and 2% PhCH=CHPh; i.e., a cage effect of 100% is observed.

## Experimental Section

**Synthesis of 2,4-Diphenylpentan-3-one.** At 0 °C, DBK (10.5 g, 50 mmol) in THF (30 mL) was added to a potassium hydride mineral oil dispersion (35%, 6.0 g, 53 mmol) suspended in THF (250 mL). After 30 min of stirring at room temperature and recooling to 0 °C, *n*-butyllithium (1.6 M, 34 mL, 54 mmol) was added by syringe. The burgundy dianion solution was stirred at 0 °C for 15 min, followed by addition of methyl iodide (15.3 g, 108 mmol) in THF (30 mL). The solution was stirred at room temperature for 10 h, followed by aqueous workup. The resulting oil was passed through a column of silica gel to remove residual hydrocarbons. The product (mixture of diastereomers) was obtained in 77% yield.

**Separation of *d,l*- and *meso*-2,4-Diphenylpentan-3-one.** The two diastereomers were separated on a Whatman Magnum 9 ODS-3 HPLC column (9.0  $\times$  50.0 cm, 15% water in methanol, 2.5 mL per min).

**Identification of *d,l*-2,4-Diphenylpentan-3-one.** One diastereomer, a viscous liquid, was identified as *d,l*-2,4-diphenylpentan-3-one by reduction to the hydrocarbon, *d,l*-2,4-diphenylpentane, via a two-step process: thioketalization with boron trifluoride etherate and ethanedithiol (room temperature, 24 h, followed by dilution with ether and water and then bicarbonate washing) followed by reduction with Raney nickel in ethanol (reflux, 18 h). The recovered 2,4-diphenylpentane was found to consist as a mixture of *d,l* and *meso* isomers (66% and 34%, respectively) by comparison with authentic diastereomers.<sup>8</sup> <sup>1</sup>H NMR (CDCl<sub>3</sub>)  $\delta$  1.24 (d,

$J = 6$  Hz, 6 H), 3.76 (q,  $J = 6$  Hz, 2 H), 7.12–7.38 (m, 10 H);  $^{13}\text{C}$  NMR ( $\text{CDCl}_3$ )  $\delta$  19.02 ( $\text{CH}_3$ ), 50.91 (CH); UV (benzene)  $\lambda$  ( $\epsilon$ ) 295 (363), 304 (327), 320 nm (93).

**Identification of meso-2,4-Diphenylpentan-3-one.** One diastereomer, a low-melting solid (mp 38.0–38.5 °C) was shown to be meso-2,4-diphenylpentan-3-one by reduction to meso-2,4-diphenylpentane by the two-step process discussed above. The recovered hydrocarbon was found to consist of a mixture of *d,l* and meso isomers (22% and 78%, respectively) by comparison with authentic diastereomers of 2,4-diphenylpentane:<sup>8</sup>  $^1\text{H}$  NMR ( $\text{CDCl}_3$ )  $\delta$  1.35 (d,  $J = 6$  Hz, 6 H), 3.87 (q,  $J = 6$  Hz, 2 H), 6.95–7.20 (m, 10 H);  $^{13}\text{C}$  NMR ( $\text{CDCl}_3$ )  $\delta$  19.27 ( $\text{CH}_3$ ), 51.51 (CH); UV (benzene)  $\lambda$  ( $\epsilon$ ) 297 (309), 305 (273), 320 nm (112).

**Synthesis of 2,4-Diphenylpentane.**<sup>8</sup> To an excess of magnesium (4.8 g, 200 mmol) in ether (100 mL) was added dropwise at room temperature 2-phenylpropyl bromide (26.7 g, 135 mmol). After spontaneous reflux subsided, the Grignard solution was refluxed for 1 h, followed by addition of acetophenone (15.6 g, 130 mmol) in ether (50 mL). The solution was refluxed for 4 h, poured onto ice water, acidified to pH 1, and extracted into ether. After drying with sodium sulfate and removal of ether, the residue was refluxed in a benzene solution with *p*-toluenesulfonic acid (0.2 g) in a Dean–Stark trap. After washing with saturated bicarbonate solution, the organic solvent was removed under vacuum. The residue was dissolved in ethanol (500 mL) and hydrogenated over platinum oxide with hydrogen entrained in a balloon. After 2 days of stirring, the solution was filtered through Celite, the solvent evaporated off, and the residue flash distilled to give 12.0 g (40% yield) of product.

**Separation of meso- and *d,l*-2,4-Diphenylpentane.** The two diastereomers were separated by preparative VPC (10% Apiezon L, 0.25 in.  $\times$  6 ft, 165 °C). Product purity was determined by capillary VPC (Carbowax 20M, 50 m, 210 °C).

**Identification of meso-2,4-Diphenylpentane.** The second eluting isomer on capillary VPC (Carbowax 20M) was identified by comparison with reported absorption and emission spectra in methylene chloride.<sup>9</sup> Specifically, considerable excimer emission (326 nm) was observed with an excitation wavelength of 260 nm.<sup>9</sup>

**Identification of *d,l*-2,4-Diphenylpentane.** This diastereomer, the first to elute, was identified by comparison with reported absorption and emission spectra in methylene chloride.<sup>9</sup> No excimer emission was observed for this isomer with an excitation wavelength of 260 nm. Only monomer benzene type emission was observed (285 nm).<sup>9</sup>

**Synthesis of 1,3-Diphenylbutan-2-one.**<sup>10</sup> To magnesium (29 g, 1.2 mol) in THF (100 mL) was added 2-bromopropane (50 g). After spontaneous initiation, additional 2-bromopropane (73 g, total 1.0 mol) in THF (300 mL) was slowly added with periodic cooling. After 30 min at reflux, the solution was cooled to 0 °C and ethyl phenylacetate (100 g, 0.6 mol) was added dropwise with stirring. After 3 h at room temperature, the reaction mixture was poured onto ice water (700 mL), acidified with concentrated HCl, and extracted into ether. The solvent was removed under vacuum and the residue redissolved in ethanol. After addition of Norit, the alcohol solution was heated to boiling and filtered through Celite to give 2,4-diphenyl-3-oxobutyric acid ethyl ester, which crystallized upon cooling to –20 °C; mp 78–79 °C (lit. mp 78 °C).<sup>11</sup> The yield was 99%.

The keto ester (54 g, 0.19 mol) in THF (150 mL) was added dropwise at 0 °C to sodium hydride (9.6 g, 50% mineral oil dispersion, 0.20 mol) suspended in THF (400 mL). After 15 min at 0 °C, *n*-butyllithium (1.6 M, 124 mL, 0.21 mol) was added. After 15 min of stirring at 0 °C, methyl iodide (31 g, 0.22 mol) in heptane (10 mL) was added. The solution was stirred at room temperature for 1 h and poured onto concentrated HCl (50 mL) previously mixed with ice water (200 mL). Ether extraction and filtration through a silica gel column gave an orange oil (35 g, 61% yield). The oil (9.5 g, 0.32 mol) was refluxed with 60% (w/v) sulfuric acid (50 mL) for 28 h. Ether extraction followed by distillation (124–126 °C, 1 mmHg) gave 1,3-diphenylbutan-2-one (4.3 g, 58% yield):  $^1\text{H}$  NMR ( $\text{CDCl}_3$ )  $\delta$  1.33 (d,  $J = 7$  Hz, 3 H), 3.59 (s, 2 H), 3.81 (q,  $J = 8$  Hz, 1 H) 6.94–7.47 (m, 10 H);  $^{13}\text{C}$  NMR ( $\text{CDCl}_3$ )  $\delta$  17.54 ( $\text{CH}_3$ ), 47.99 ( $\text{PhCH}_2$ ), 52.06 ( $\text{PhCH}$ ); UV (0.05 M SDS)  $\lambda$  ( $\epsilon$ ) 260 (358), 290 nm (244); (0.05 M HDTCl)  $\lambda$  ( $\epsilon$ ) 260 (897), 290 nm (364).

**Synthesis of 1,3,4-Triphenylbutan-2-one.** To a suspension of sodium hydride (2.6 g, 50% mineral oil dispersion) in THF (25 mL) was added dropwise at 0 °C 2,4-diphenyl-3-oxobutanenitrile<sup>12</sup> (11.8 g, 50 mmol) in THF (100 mL). After 15 min at room temperature, the solution was cooled to 0 °C and *n*-butyllithium (35 mL, 1.6 M, 55 mmol) in hexane

was added. After 15 min at room temperature, and cooling to 0 °C, benzyl chloride (7.6 g, 60 mmol) in THF (30 mL) was added, followed by stirring at room temperature for 2 h. The solution was poured onto water (200 mL) and the organic layer removed. Evaporation gave a golden viscous oil that solidified upon standing. Trituration with hexane gave 2,4,5-triphenyl-3-oxopentanenitrile (13.1 g, 40 mmol, 81% yield).

The product from above (9 g, 27 mmol) was refluxed with 60% (w/v) sulfuric acid for 24 h.<sup>13</sup> After being poured onto ice and extracted with ethyl acetate, evaporation of the organic solvent gave an oil, which crystallized from hot hexane to give 1,3,4-triphenylbutan-2-one (6.7 g, 81% yield). Additional recrystallizations from ethanol–water mixtures yielded a purer product: mp 75.0–76.0 °C (lit. mp 73–74.5 °C,<sup>7</sup> 74–75.5 °C,<sup>14</sup> 77–78 °C<sup>15</sup>);  $^1\text{H}$  NMR ( $\text{CDCl}_3$ )  $\delta$  ( $\text{PhCH}_2\text{H}_m\text{CH}_x(\text{Ph})\text{CO}-$ ) 2.84 ( $\text{H}_m$ , dd,  $J_{am} = 14$  Hz,  $J_{mx} = 7$  Hz, 1 H), 3.38 ( $\text{H}_a$ , dd,  $J_{am} = 14$  Hz,  $J_{ax} = 8$  Hz, 1 H), 4.00 ( $\text{H}_x$ , dd,  $J_{ax}$ ,  $J_{mx}$ , 1 H), 3.51 ( $\text{PhCH}_2\text{CO}-$ , s, 2 H), 6.82–7.44 (m, 15 H); UV (isooctane)  $\lambda$  ( $\epsilon$ ) 243 (605), 249 (903), 255 (1152), 260 (1033), 298 (308), 313 nm (188) (lit. UV (cyclohexane)<sup>16</sup>)  $\lambda$  ( $\epsilon$ ) 260 (615), 298 nm (332)).

**Homogeneous and Micellar Solutions.** Micelle solutions were prepared by overnight stirring of the ketone (1 mM) in detergent solutions of SDS (50 mM), HDTCl (50 mM), or HDTBr (25 mM). The detergents were previously purified by recrystallizations. The micelle solutions were nitrogen purged, followed by capping the Pyrex test tube with Teflon-lined screw caps and securing with parafilm. Homogeneous solutions (1–10 mM) were typically vacuum degassed by three freeze–thaw cycles ( $10^{-5}$  mmHg) and sealed by flame under vacuum. Both homogeneous and micellar solutions were irradiated by using a medium-pressure Hg lamp, quartz immersion well, and a potassium chromate (0.272 g per L) in 0.1% (w/v) sodium carbonate solution (313-nm filter solution). Quantum yields for micellar solutions were determined relative to the disappearance of dibenzyl ketone by utilizing solutions of dibenzyl ketone in benzene.<sup>6</sup>

**Preparation of Porous Glass Samples.** Corning borosilicate glass no. 7930 were cut into squares (10 mm  $\times$  10 mm  $\times$  3 mm) weighing between 0.250 and 0.500 g per square. The porous glass was routinely cleaned by soaking in concentrated nitric acid for several days, continued washing with water until neutral, and vacuum drying for several days with a rough vacuum pump. No changes in results were observed when the drying procedure was expedited by utilizing vacuum drying at 150 °C. Ketones were applied to the glass in hydrocarbon solvents (benzene or isooctane) either by syringe or soaking, dried under vacuum, and sealed in Pyrex tubes after degassing at  $10^{-5}$  mmHg for at least 0.5 h. In general, the solvent can be observed visually as it is being pumped off the glass within this time period, but residual solvent remains (VPC analysis) even after 24 h of drying time. Irradiations appeared to be insensitive to the length of drying.

**Preparation of TLC, RPTLC, and Porous Silica Samples.** Whatman-supplied thin-layer chromatography plates (K6 and RPK5) and porous silica were utilized as received. The samples, usually applied by syringe (50  $\mu\text{L}$ ) as hydrocarbon solutions, were added to the glass-backed silica supports previously cut into 10 mm  $\times$  20 mm rectangles. They were dried and sealed under vacuum as described for the porous glass samples.

**Irradiations of Glass and Silica-Support Samples.** The Pyrex test tubes containing the porous glass, porous silica, silica gel, or TLC/RPTLC plates were irradiated with either a 450-W medium-pressure Hg lamp using the potassium chromate in carbonate filter solution discussed previously or with a 1000-W Hg–Xe Oriel lamp utilizing a 10-cm filter solution to isolate the 313-nm line ( $\text{KCrO}_4$ , 0.027 g per L in 0.01% (w/v) sodium carbonate). A quartz Dewar filled with dry ice–alcohol was utilized for all low-temperature irradiations. The photolysis time was typically 10 min, 10–20 min, and 1 h for the micelle solutions at ambient temperature, glass and silica-support samples at ambient temperature, and the support samples at low temperature, respectively.

**Workup and Analytical Techniques.** The micellar solutions were extracted with ether by utilizing centrifugation of the screw-cap test tubes to quickly separate the organic and aqueous layers. The supported samples were soaked in methylene chloride for at least 10 min to extract out photoproducts. The micellar extracts were dried over sodium sulfate, evaporated under a nitrogen stream, diluted in methylene chloride, redried, and filtered through a pipet filled with glass wool. Finally, all samples were dried under a nitrogen stream to approximately 100  $\mu\text{L}$  and analyzed by VPC. A Varian 3700 capillary vapor-pressure chromat-

(9) Bokoboza, L.; Jasse, B.; Monnerie, L. *Eur. Polym. J.* **1977**, *13*, 921.

(10) Thompson, H. W.; Huegi, B. S. *J. Chem. Soc., Chem. Commun.* **1973**, 636. Posner, G. H.; Sterling, J. J. *J. Am. Chem. Soc.* **1973**, *95*, 3076.

(11) Conant, J. B.; Blatt, A. H. *J. Am. Chem. Soc.* **1929**, *51*, 1227.

(12) Coan, S. B.; Becker, E. I. "Organic Syntheses"; Wiley: New York, 1955; Collect. Vol. III, p 174.

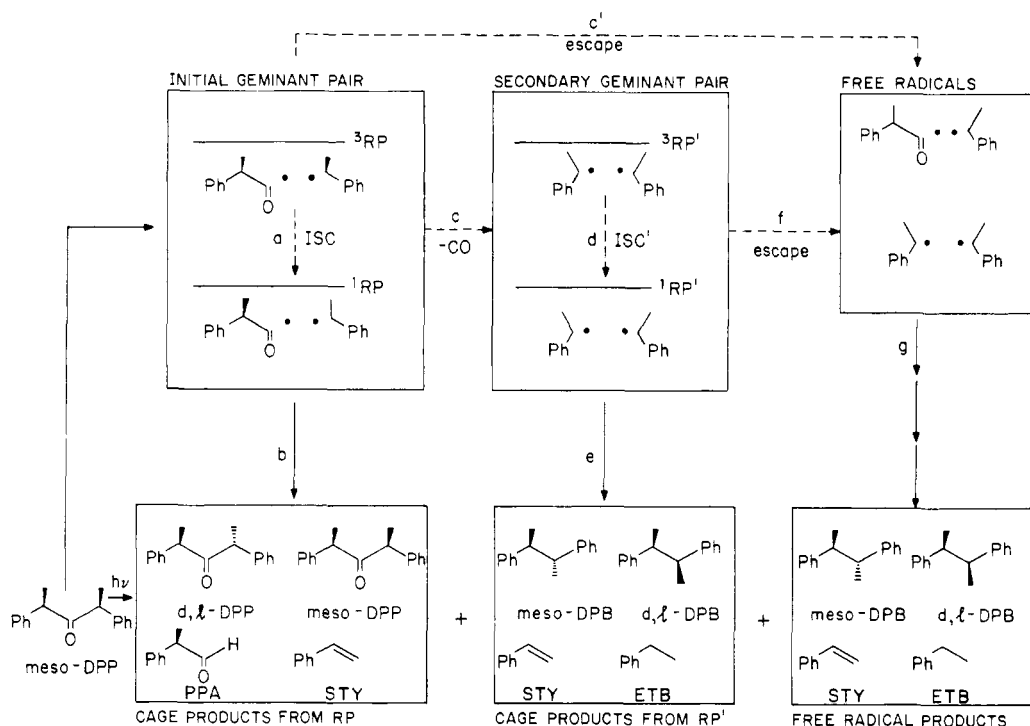
(13) Coan, S. B.; Becker, E. I. "Organic Syntheses"; Wiley: New York, 1955; Collect. Vol. III, p 176.

(14) McKenzie, A.; Rogers, R. *J. Chem. Soc.* **1927**, 571.

(15) Bettzieche, F.; Erhlich, A. *J. Physiol. (London)* **1925**, *150*, 177.

(16) MacKenzie, S.; Marsocci, S. F.; Santurri, P. R. *J. Org. Chem.* **1963**, *28*, 717.

Scheme I



graph was utilized, usually with a Hewlett-Packard methyl silicone fused silica column (50 m) at 210 °C.

**CIDNP Experiments.** A Bruker WP-80 FT-NMR was utilized for the polarization studies. A quartz light rod was permanently fixed to a proton probe within the NMR magnet. The light source was a 1000-W Hg-Xe Oriel lamp with a 10-cm water filter bath.

### Discussion

**Working Mechanism.** Scheme I provides a working mechanism, based on the well-established mechanism for photolysis of dibenzyl ketone<sup>6</sup> and with *meso*-DPP as a specific example, which serves as a basis for the discussion of our results. We assume that, in analogy to the results with DBK, a caged, geminate triplet radical pair ( $^3RP$ ) is produced by photoexcitation of *meso*-DPP (via a  $S_1 \rightarrow T_1 \rightarrow ^3RP$  pathway). We also assume that of the intersystem crossing (ISC) steps, a ( $^3RP \rightarrow ^1RP$ ) and c ( $^3RP' \rightarrow ^1RP'$ ) will be inhibited relative to other pathways, because in a field of sufficient strength, ISC from the  $T_+$  and  $T_-$  states of the radical pairs is inhibited due to the Zeeman splitting of the triplet sublevels.

From Scheme I, the observed products may be grouped into three types: type 1, cage products derived from recombination and disproportionation reactions of the primary geminate radical pair; type 2, cage products derived from recombination and disproportionation reactions of the secondary geminate radical pair produced by decarbonylation; and type 3, products derived from recombination and disproportionation of free radicals.

The environment is expected to play a major role in determining the competition between the formation of cage products from geminate radical pairs and the escape of the geminate radical pairs to form free radicals. If the environment imposes constraints, by any mechanism, of the diffusional displacements of the components of geminate radical pairs required to produce free radicals, the efficiency of geminate radical pairs undergoing cage reactions will be enhanced. Such environments are termed "super cages" because of their superior ability to contain a radical pair in a restricted space (cage) compared to the cage produced by a fluid homogeneous solvent.

Temperature should also play a role in determining the competition between the formation of cage products originating from the initial geminate pair and cage products originating from the secondary geminate pair. This temperature effect is expected because the rate of decarbonylation (path c) is known to be

temperature dependent.<sup>17</sup> Thus, the competition between path c and paths a and c' will differ as the temperature is varied. On the other hand, temperature effects on the reactions of caged radical pairs are generally small.<sup>18</sup>

Finally, the application of an external magnetic field will cause a significant variation of products if path c' is not dominant. This requirement arises from the need for preservation of spin correlation in the radical pair. Thus, magnetic field effects are more likely for radical pairs in super-cage environments than the solvent cages of homogeneous solvents because path c' usually dominates in the latter environments.

**Environmental Effects on the Photolysis of *meso*-DPP at a Given Temperature.** The data in Table I are consistent with the postulate that (compared to homogeneous solvents) SDS micelles, porous silica, porous glass, silica on TLC, and reverse-phase silica on TLC provide super-cage environments for the geminate radical pairs produced in the photolysis of *meso*-DPP. For example, the type I products (*d,l*-DPP and PPA) that are formed in trace amounts in pentane are formed in significant quantities in the super-cage environments. The *s* values for isomerization (Table II) indicate that (at 27 °C) the order of the cage effect is porous glass > SDS micelles > HDTCl micelles. The ratio of disproportionation to coupling of a given radical pair in homogeneous solution is generally not very sensitive to variations in solvent.<sup>19</sup> However, a substantial variation in the ratio of combination to disproportionation is observed, at a given temperature, as the super-cage environment is varied (Table VI).

**Temperature Effects on the Photolysis of *meso*-DPP in a Given Environment.** The influence of temperature on the products of photolysis of *meso*-DPP are summarized in Tables I, V, and VI. It is noted that for pentane solvent as the environment, the effect of temperature on the product ratio is minor (93% and 90% DPB at 27 and -77 °C, respectively). On the other hand, there is a general increase in the type I products in the super-cage systems (Tables I and V). This trend is consistent with Scheme I if path

(17) Robbins, W. K.; Eastman, R. H. *J. Am. Chem. Soc.* **1970**, *92*, 6076, 6077. Bruntan, G.; McBay, H. C.; Ingold, K. U. *Ibid.* **1977**, *99*, 4447. Paul, H.; Fischer, H. *Helv. Chim. Acta* **1973**, *56*, 1575.

(18) Gibian, M. J.; Corley, R. C. *Chem. Rev.* **1973**, *73*, 441.

(19) Dixon, P. S.; Stefani, A. P.; Szwarc, M. *J. Am. Chem. Soc.* **1963**, *85*, 2551. Bennet, J. E.; Mile, B.; Thomas, A.; Ward, B. *Adv. Phys. Org. Chem.* **1970**, *8*, 1. Sheldon, R. A.; Kochi, J. K. *J. Am. Chem. Soc.* **1970**, *92*, 4395.

**Table V.** Temperature Effects from Irradiation of *meso*-DPP under Various Conditions (Percent Increase (Decrease) of Product Formation Relative to Pentane)<sup>a</sup>

product	temp, °C	environment				RPTLC
		SDS	porous glass	porous silica	TLC	
<i>d,l</i> -DPP	27	1500	1500	1500	2300	900
<i>d,l</i> -DPP	-77		8900		7900	7700
2-PPA	27	500	300	100	300	300
2-PPA	-77		7400		5900	7400
ETB	27	200	166	0	0	66
ETB	-77		25		(50)	25
STY	27	166	100	66	66	133
STY	-77		300		200	300

<sup>a</sup> With the data from Table I, values represent the percent change for product formation relative to the amount obtained in pentane at the corresponding temperature (e.g., for percent increase in styrene formation on RPTLC at -77 °C,  $([20 - 5]/5) \times 100 = 300\%$ ). The error is  $\pm 25\%$ .

**Table VI.** Disproportionation Products with Photolysis of *meso*-DPP

environment	isomer	temp, °C	% DPB <sup>a</sup>	% disp <sup>a</sup>	% PPA <sup>b</sup>	% ETB <sup>b</sup>
pentane	<i>d,l</i> + <i>meso</i>	27	97 <sup>c</sup>	3	5	95
pentane	<i>meso</i>	27	97	3	9	91
pentane	<i>d,l</i> + <i>meso</i>	-77	93	7	5	95
pentane	<i>meso</i>	-77	93	7	5	95
SDS	<i>meso</i>	27	86	14	24	76
porous glass	<i>d,l</i> + <i>meso</i>	27	91	9	20	80
porous glass	<i>meso</i>	27	90	10	21	79
porous glass	<i>d,l</i> + <i>meso</i>	-77 <sup>d</sup>	59	41	72	28
porous glass	<i>meso</i>	-77 <sup>d</sup>	57	43	75	25
PorSilica (122 Å)	<i>d,l</i> + <i>meso</i>	27	92	8	21	79
PorSilica (122 Å)	<i>meso</i>	27	94	6	27	73
PorSilica (20 Å)	<i>d,l</i> + <i>meso</i>	27	86	14	21	79
PorSilica (122 Å)	<i>d,l</i> + <i>meso</i>	-77 <sup>d</sup>	56	44	88	12
PorSilica (122 Å)	<i>meso</i>	-77 <sup>d</sup>	56	44	88	12
PorSilica (20 Å)	<i>d,l</i> + <i>meso</i>	-77 <sup>d</sup>	45	55	78	22
TLC	<i>meso</i>	27	94	6	42	58
TLC	<i>meso</i>	-77 <sup>d</sup>	69	31	82	18
RPTLC	<i>meso</i>	27	93	7	35	65
RPTLC	<i>meso</i>	-77 <sup>d</sup>	54	46	78	22

<sup>a</sup> % disp is defined as  $([PPA] + [ETB])/([PPA] + [ETB] + [DPB])$ . % DPB is  $100 - \% \text{ disp}$ . <sup>b</sup> % PPA is defined as  $([PPA])/([PPA] + [ETB])$ . % ETB is  $100 - \% \text{ PPA}$ . <sup>c</sup> These values are reproducible to within at least 5% of their reported magnitude.

<sup>d</sup> Refers to the temperature of the bath the samples were immersed in.

c is subject to a greater relative decrease in rate as the temperature is lowered. Such a situation allows path b (leading to type I products) to increase.

In Table VI, the influence of temperature on the percent recombination and disproportionation products is summarized. In pentane, the effect of temperature is minor, but in the super-cage systems, significant temperature variations are observed. Scheme I does not deal directly with the recombination/disproportionation ratio since these are the ultimate products of radical pairs, whatever the pathways by which they react.

We note that the observed increase in photoisomerization with decreasing temperature implies that at -77 °C radical rotational motion is not strongly inhibited. However, the observation of cage effects on benzylic-benzylic radical pair recombination for substituted dibenzyl ketone irradiated on porous glass implies a constraint to translational motion within the time frame of radical-pair intersystem crossing. These interpretations parallel recent observations of cumyl radical rotational and translational motion on adsorbed to silica surfaces.<sup>20</sup> The observed small increase in styrene yields during photolysis of DPP in pentane (Table VI)

is consistent with the known temperature dependence of disproportionation/recombination relative efficiencies for dicumyl radical pairs.<sup>21</sup> In fact, the amount of PPA that accompanies styrene formation decreases 44% in pentane photolysis over the temperature range studied.

It is interesting to note that at room temperature, the disproportionation of di-*sec*-phenethyl radical pairs increases, relative to radical-pair coupling, in micelles and porous silicates when compared to pentane irradiations (Table VI). The increase (100–350%) may reflect the more substantial orientational restraints that are imposed upon radical-pair coupling relative to disproportionation after free rotation and radical separation has taken place.<sup>21</sup>

**Magnetic Field Effects on the Photolysis of *meso*-DPP.** Table II presents data on the influence of an applied magnetic field on the  $s$  values for isomerization to *d,l*-DPP. For each super-cage system studied (SDS micelles, HDTCl micelles, and porous glass), there is a significant decrease in  $s$  values when a field (3000 G) is applied. From Scheme I, an explanation is found if the field decreases path a relative to path c. Under such conditions, fewer geminate RP radicals undergo cage reaction.

**Magnetic Field Effects on the Photolysis of  $\alpha$ -MeDBK.** The magnitude of the cage effect in the photolysis of  $\alpha$ -MeDBK is significantly magnetic field dependent in all super-cage environments (Table III). On the basis of Scheme I (replacing PhCHCH<sub>3</sub>COCH<sub>2</sub>Ph radical pairs for RP and PhCHCH<sub>3</sub>CH<sub>2</sub>Ph radical pairs for RP'), this magnetic field effect would arise if path d (ISC) were inhibited relative to path f (escape). Under such conditions, a greater production of free radicals would be produced and a smaller cage effect would be observed.

The cage values obtained with irradiation of  $\alpha$ -MeDBK ranges from 9% to 47%, depending on the surface environment and temperature utilized. Although these values are lower than the corresponding cage effects in SDS and HDTCl micellar solution, the observation of magnetic field effects of similar magnitude suggest that the same competition between radical-pair escape and recombination operates in micelles as in porous silicates.<sup>22</sup>

The cage effects in micelles for benzylic-type radical pairs have been previously reported with the use of para-substituted dibenzyl ketone substrates.<sup>6</sup> It is interesting to note that the cage values for  $\alpha$ -MeDBK (71% and 74% in HDTCl and SDS) are greater than those reported for *p*-MeDBK<sup>23</sup> (50% and 30% in HDTCl and SDS, respectively). Since the hydrophobicity for both compounds should be similar on the basis of carbon content, we speculate that the greater sum of hyperfine coupling constants for the  $\alpha$ -substituted compound is responsible for the increase in the cage effect relative to the para-substituted isomer. Utilization of CuCl<sub>2</sub> as a selective aqueous scavenger in HDTCl solutions was successful in determining the cage values for diphenylethane formation with the photolysis of DPP (67% and 23% at 0 and 3000 G, respectively). This technique for estimating cage values for symmetrical radical pairs was demonstrated previously with DBK and *p*-MeDBK photolysis in micellar solutions.<sup>24</sup>

**Photolysis of TPB. Environment and Temperature Effects.** The results of our investigation of irradiation of TPB are also consistent with the general features of Scheme I. At low temperatures, porous glass and silica irradiations lead to a 240% and 170% increase, respectively, in stilbene formation (disproportionation) relative to low-temperature homogeneous-solvent photolysis. This may reflect the different escape rates from the primary radical pair cage (corresponding to the analogous RP in Scheme I). However, the observed decrease in disproportionation with irradiation of solid samples (70% decrease) suggests that little translational or rotational displacement can take place in the rigidly solid state. The large cage values (100%) support the lack of translational motion in the solid state.

(21) Nelson, S. F.; Bartlett, P. D. *J. Am. Chem. Soc.* **1966**, *88*, 137.

(22) Avnir, D.; Johnston, L. J.; de Mayo, P.; Wong, S. K. *J. Chem. Soc., Chem. Commun.* **1981**, 958.

(23) Weed, G. Ph.D. Dissertation, Columbia University, 1981.

(24) Turro, N. J.; Chow, M.-F.; Chung, C.-J.; Weed, G. C.; Kraeutler, B. *J. Am. Chem. Soc.* **1980**, *102*, 4843.

(20) Leffler, J. E.; Zupancic, J. J. *J. Am. Chem. Soc.* **1980**, *102*, 259.

## Conclusion

In a previous publication,<sup>25</sup> it was pointed out that CIDNP polarization in homogeneous photolysis often predicts the appearance of products in significant yields with micellar irradiations in contrast to the insignificant yields in homogeneous photolysis analysis. In this work, we observe that PPA and DPP stereoisomers are indeed formed in substantial amounts during the photolysis of DPP in micelle solutions (and in other super-cage environments) despite the fact that these products are present to less than 1% of total photoproducts in pentane irradiations. The styrene polarization in the CIDNP spectrum (Figure 1) produced by irradiation of DPP in C<sub>6</sub>D<sub>6</sub> is consistent with the operation of two disproportionation mechanisms for formation of styrene. In pentane, the amount of PPA that accompanies styrene formation is twenty times less than the corresponding ethylbenzene formed, suggesting that most of the styrene arises from path c' followed by path g. However, in SDS and porous silicates (Table VI), about 20-40% of the styrene produced is accompanied by

PPA formation (the values are 70-80% for low-temperature photolysis), suggesting that path b to styrene is becoming significant due to the super-cage environment.

Finally, we note that these studies have demonstrated that the magnetic field effects for radical-pair recombinations are not restricted to only micellar solutions but are more like a general property of the restricted space provided by super-cage environments.<sup>26</sup> This confirms the notion that a magnetic field effect on micelle structures is not the dominant cause for effects previously noted in DBK <sup>13</sup>C-enrichment<sup>6</sup> and benzylic radical pair coupling studies.<sup>23</sup>

**Acknowledgment.** We thank the National Science Foundation for its generous support of this research. We also thank Drs. Gary Lehr and Eugene Sitzmann for helpful discussions.

**Registry No.** meso-DPP, 84454-38-6; d,l-DPP, 84454-39-7; TPB, 62640-72-6; α-MeDBK, 13363-25-2; PhCH<sub>2</sub>COCH<sub>2</sub>Ph, 102-04-5; PhCHCOCHPh·Li<sup>+</sup>·K<sup>+</sup>, 64020-30-0; SDS, 151-21-3; HDTCl, 112-02-7.

(25) Lehr, G.; Turro, N. J. *Tetrahedron* 1981, 37, 3411.

(26) Buchachenko, A. L.; Tarasov, V. F.; Mal'tsev, V. I. *Russ. J. Phys. Chem. (Engl. Transl.)* 1981, 55, 936.

## Cyclic and High Polymeric *nido*-Carboranylphosphazenes as Ligands for Transition Metals<sup>1</sup>

Harry R. Allcock,\* Angelo G. Scopelianos, Robert R. Whittle, and Norris M. Tollefson

Contribution from the Department of Chemistry, The Pennsylvania State University, University Park, Pennsylvania 16802. Received May 6, 1982

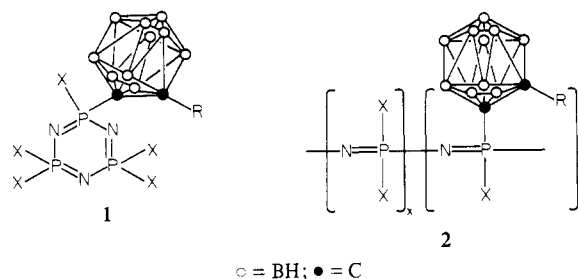
**Abstract:** 1-Methyl-1-(2-propynyl)-3,3,5,5-tetrachlorocyclotriphosphazene (**6**) reacts with bis(acetonitrile)-decaborane to yield 1-methyl-1-[(*o*-carboranyl)methylene]-3,3,5,5-tetrachlorocyclotriphosphazene (**7**). Species **7** was converted by base to the *nido*-carboranyl anion or dianion derivatives, which react with Rh(PPh<sub>3</sub>)<sub>3</sub>Cl or with Mo(CO)<sub>6</sub> or W(CO)<sub>6</sub> to form the appropriate (metallo-carboranyl)phosphazene derivatives (**10** or **12**). Compound **7** polymerizes when heated, and the high polymeric analogues (**13**, **14**, and **16**) behave in a similar manner to the cyclotriphosphazene derivatives in the formation of metallocarboranyl derivatives. Species **7** is unusual in its reaction with piperidine. The four halogen atoms are replaced by piperidino groups, and a boron atom is removed from the cage, but an internal counterion at skeletal nitrogen is generated rather than the expected piperidinium ion. An X-ray structural investigation of this species (**8**) confirmed the presence of a planar cyclotriphosphazene ring linked to the carboranyl unit through a methylene spacer group. A proton was connected to the phosphazene skeletal nitrogen atom furthest from the carboranyl group. The P-N bonds adjacent to the site of the carborane attachment were of normal length (1.575 Å), but the two bonds furthest from this site were exceptionally long (1.68 Å), presumably a consequence of ring protonation.

Complexes between *nido*-carboranyl structures and transition metals are well-known.<sup>2-4</sup> Recently we reported the first syntheses of *closo*-carboranes linked through C-P bonds to both cyclic and high polymeric phosphazenes.<sup>5</sup> In this present paper, we explore the prospect that *nido*-anion-species derived from carboranyl-phosphazenes might function as ligands for transition metals. Such compounds may be of interest as high-temperature, immobilized-catalyst species or as prototypes for polymers with unusual electrical behavior.

The objectives of this study were (1) to determine if neutral carboranylphosphazenes could be converted to the *nido*-anion

species by strategies similar to those employed for the free carborane,<sup>3</sup> without decomposition of the phosphazene unit; (2) to identify the site of B-H bond loss from the neutral carboranyl unit; (3) to determine if a *nido*-carboranylphosphazene anion would function as a π ligand for transition metals; (4) to deduce if the phosphazene unit (with its σ-donor nitrogen atoms) might interfere with the metal coordination process; and (5) to explore the applicability of this chemistry to high polymeric analogues.

In the earlier work from our laboratory,<sup>5</sup> compounds of types **1** and **2** were prepared, where R = Me or Ph and X = Cl or



(1) This paper is part of a series on phosphorus-nitrogen ring systems and high polymers. For the previous paper, see: Allcock, H. R.; Lavin, K. D.; Tollefson, N. M.; Evans, T. L. *Organometallics* 1983, 2, 267.

(2) Hawthorne, M. F. *Organomet. Chem.* 1975, 100, 97.

(3) Hawthorne, M. F.; Young, D. C.; Garrett, P. M.; Owen, D. A.; Schwerin, S. G.; Tebbe, F. N.; Wegner, P. A. *J. Am. Chem. Soc.* 1968, 90, 862.

(4) Hawthorne, M. F.; Young, D. C.; Andrews, T. D.; Howe, D. V.; Pilling, L. R.; Pitts, A. D.; Reintjes, M.; Warren, L. F., Jr.; Wegner, P. A. *J. Am. Chem. Soc.* 1968, 90, 879.

(5) Scopelianos, A. G.; O'Brien, J. P.; Allcock, H. R. *J. Chem. Soc., Chem. Commun.* 1980, 198. Allcock, H. R.; Scopelianos, A. G.; O'Brien, J. P.; Bernheim, M. Y. *J. Am. Chem. Soc.* 1981, 103, 350.

OCH<sub>2</sub>CF<sub>3</sub>. These compounds formed the starting point for our